

Ratchetlike pulse controlling the Fermi deceleration and hyperacceleration

Cesar Manchein¹, and Marcus W. Beims^{1,y}¹Departamento de Física, Universidade Federal do Paraná, 81531-990 Curitiba, PR, Brazil

Using an ac driven asymmetric pulse we show how the Fermi acceleration (deceleration) can be controlled. A deformed sawtooth (Ratchetlike) pulse representing the moving wall in the static Fermi-Ulam model is considered. The time integral from the pulse over one period of oscillation must be negative to obtain deceleration and positive to obtain hyperacceleration. We show that while the decelerated case is chaotic, for the hyperaccelerated case the Lyapunov exponents converge to zero. Numerical simulations indicate that the hyperaccelerated case is ergodic in velocity space. Switching between different pulse deformations we are able to control the particle acceleration. Results should be valid for any pulse for which the time integral can be manipulated between positive and negative values.

Keywords: Fermi acceleration, Control, Ratchet

Many years ago Enrico Fermi [1] suggested an acceleration mechanism of cosmic ray particles interacting with a time dependent magnetic field. Later on different versions of the original model for the Fermi acceleration were proposed. In the first one, the Fermi-Ulam (FU) model, a bouncing particle moves between a fixed surface and a parallel oscillating surface [2]. This model was shown to be chaotic [3, 4]. In order to improve simulations a simplified version of the FU model was proposed [3], called the static wall model. It ignores the displacement of the moving wall but keeps the essential information for the momentum transfer as the wall was oscillating. This static model was discussed in many aspects [3, 5, 6, 7], even for circular billiards [8]. Usually invariant curves in the phase space, found for higher velocities, prevent the particle to increase its kinetic energy without bounds. Recently the hopping wall approximation was proposed [9, 10] which takes into account the effect of the wall displacement, and allows the analytical estimation of the particle mean velocity. Compared to the simplified static model, the particle acceleration is enhanced. The second kind of Fermi accelerated model was proposed in 1977 by Pustyl'nikov [11], who considered a particle on a periodically oscillating horizontal surface in the presence of a gravitational field. The above topics got attention in various areas of physics, ranging from nonlinear physics [3, 4, 5, 6, 7, 8, 9, 10], atom optics [12, 13, 14], plasma physics [15, 16] to astrophysics [17, 18, 19].

In this paper we use an ac driven asymmetric pulse to control the acceleration (deceleration) in the simplified FU model. The pulse is a deformed sawtooth driving law for the moving wall. This Ratchetlike pulse differs from the ac driven asymmetric pulses (symmetric sawtooth) used for the Fermi acceleration in the early work of Lichtenberg et al. [3] and proposed recently to control the motion of magnetic flux quanta [20] and to analyze the relative efficiency of mechanism leading to increased acceleration in the hopping wall approximation [10]. In the simplified Fermi model [3] the particle is free to move between the elastic impacts with the walls. Consider that the moving wall oscillates between two extrema with amplitude v_0 . The gravitational force is considered zero. The system is described by a map $M_{1(2)}(V_n; \varphi_n) = (V_{n+1}; \varphi_{n+1})$ which gives, respectively, the velocity of the particle, and the phase of the moving wall, immediately after the particle suffers a collision with the wall. Considering dimensionless variables the FU map with the deformed sawtooth wall is written as

$$M_1 : \begin{cases} V_{n+1} = V_n + \frac{v_0}{1} (\varphi_n - 1) ; \\ \varphi_{n+1} = \varphi_n + \frac{(1 + \varphi_2)}{V_{n+1}} \mod (1 + \varphi_2); \end{cases} \quad (1)$$

for $\varphi_n < 1$, and

$$M_2 : \begin{cases} V_{n+1} = V_n + \frac{v_0}{2} (\varphi_n - 1) ; \\ \varphi_{n+1} = \varphi_n + \frac{(1 + \varphi_2)}{V_{n+1}} \mod (1 + \varphi_2); \end{cases} \quad (2)$$

for $\varphi_n \geq 1$, where n is the iteration number and φ is the maximum distance between the walls. Since in this simplified model the displacement of the moving wall is ignored, the modulus function is used to avoid errors due to successive collisions which may occur in the original model. In other words, if after a collision with the wall the particle continues to have a negative velocity (a successive collision will occur in the original model), the particle moves beyond the wall. The modulus for the velocity injects the particle back and fixes the problem.

The time asymmetry of the oscillating wall in Eqs. (1) and (2) is controlled by varying the parameters $(\eta_1; \eta_2)$. The deformed sawtooth (Ratchetlike) is obtained when $\eta_1 \neq \eta_2$. Figures 1 (a)–(c) show the time behavior of the oscillating

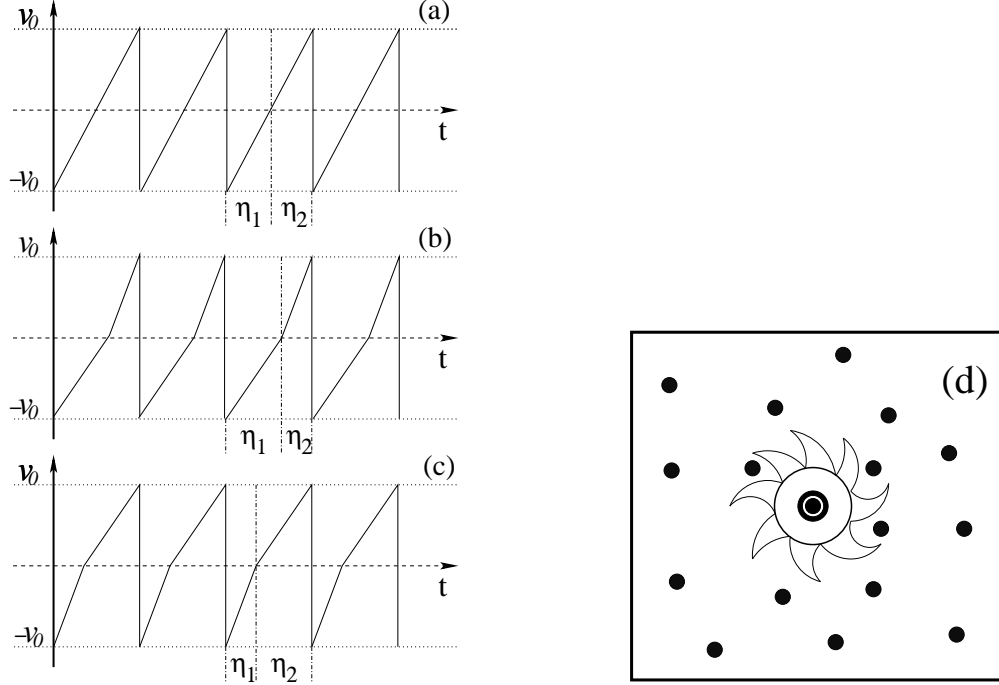


FIG. 1: (a)–(c) The shape of the pulses used in the simulations. The deformed sawtooth effect is obtained when $\eta_1 \neq \eta_2$. For (a) $\eta_1 = \eta_2 = 0$ we have the symmetric accelerated case A, (b) $\eta_1 < \eta_2$ we have the deformed desaccelerated case D and (c) $\eta_1 > \eta_2$ the deformed hyperaccelerated case H. (d) Illustration of a mechanical device which mimics the effect of the soft version of the pulses from (b)–(c). The ratchetlike cylinder may rotate clockwise and counter-clockwise.

wall (the pulse) for different values of the asymmetry $\eta_2 - \eta_1$. The deformed sawtooth pulse is obtained when $\eta_1 \neq \eta_2$. Such pulses can be easily obtained from pulse generators. As we will see we obtain three kind of accelerations: For $\eta_1 = \eta_2 = 0$ we have the symmetric accelerated case A [Fig. 1 (a)]; For $\eta_1 < \eta_2$ we have the deformed decelerated case D [Fig. 1 (b)]; and for $\eta_1 > \eta_2$ the deformed hyperaccelerated case H [Fig. 1 (c)]. Figure 1 (d) shows a very simple example of a mechanical device which generates a similar effect as the deformed sawtooth. Imagine many particles colliding elastically with the walls inside the square box, and a ratchet cylinder rotating at the center. The rotating ratchet cylinder mimics the wall oscillation of the deformed sawtooth from Fig. 1 (b)–(c). When an external motor starts to rotate the ratchet cylinder counter-clockwise, particles are hyperaccelerated. After that the motor starts to rotate clockwise and the hyperaccelerated particles are decelerated. A similar mechanical device was used for micromotors in a bacterial bath [21].

Numerically we reckon the average particles velocity at a given time n from

$$\langle v_i(n) \rangle = \frac{1}{n+1} \sum_{i=0}^{X^n} \frac{1}{X} \sum_{j=1}^X V_{n,j}; \quad (3)$$

where the index i refers to the i th iteration of the sample j , and X is the number of initial conditions. The average velocity $\langle v_i \rangle$ for the three cases A; H; D mentioned above are shown in Fig. 2. We iterate the map (1) or (2) for times $n = 1 \cdot 10^3$, and 3000 initial conditions in the interval $0 < V < 10^3$ and $0 < \eta_1 + \eta_2 < 1$. Figure 2 shows the phase space (on the left) and mean velocity (on the right) for the cases A : $\eta_1 = \eta_2 = 0$ in Figs. 2 (a)–(b); H : $\eta_1 = 0.01$ in Figs. 2 (c)–(d); and D : $\eta_1 = 0.01$ in Figs. 2 (e)–(f). First observation is that the accelerated mode can be observed in the case A. As the particle velocity increases, regular islands are observed and $\langle v_i \rangle$ increases slowly until $V \approx 10$. These regular islands prevent the particle velocity to increase very fast. It is worth to mention that all initial conditions start inside the chaotic region at low velocities. The growth rate of $\langle v_i \rangle$ depends on the number of regular islands inside the phase space. This is an expected result since this case is similar to the simplified model studied by Lichtenberg

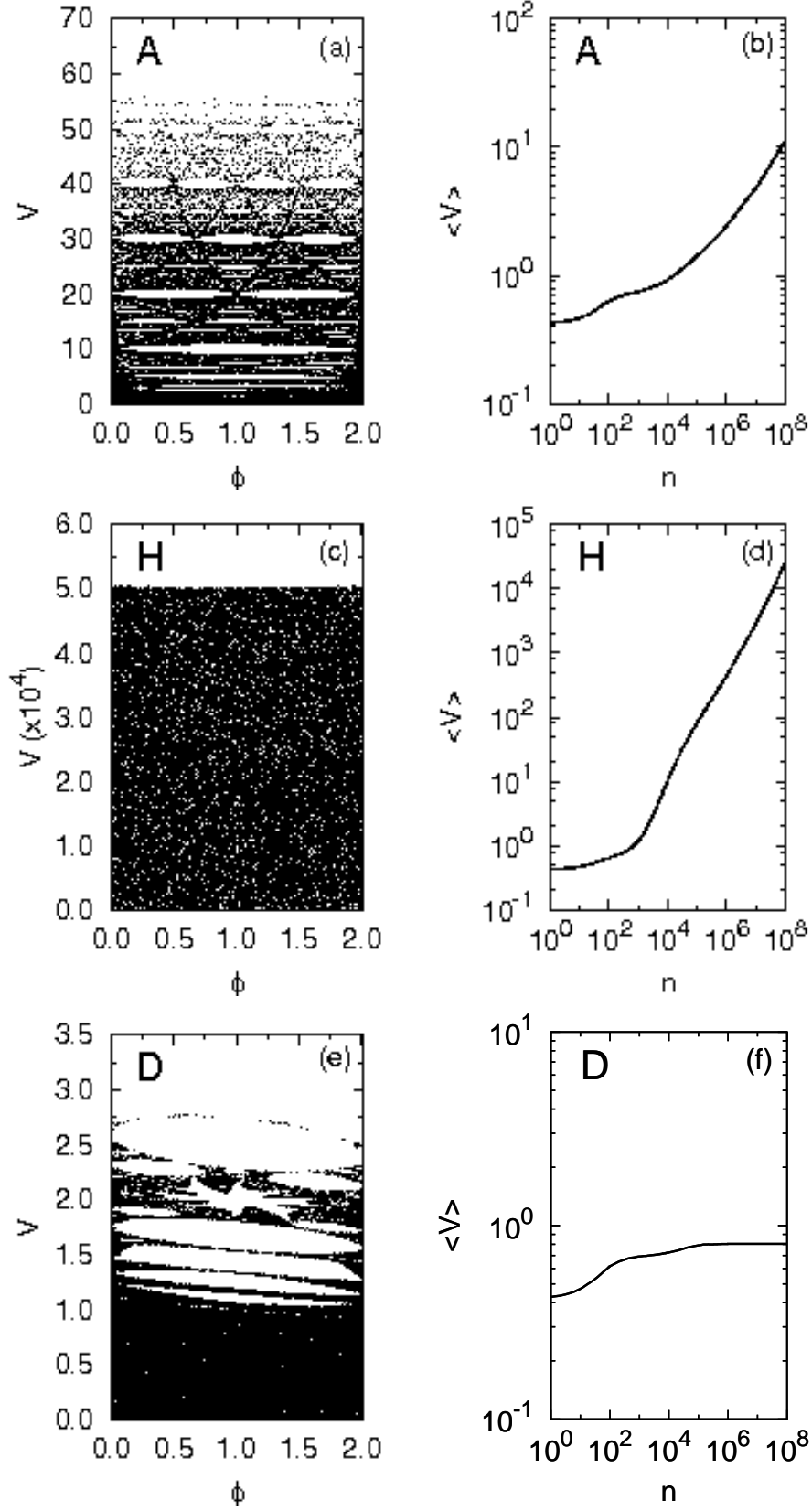


FIG. 2: Evolution of 50 chaotic orbits on the phase space V versus ϕ for the parameters $\omega = 10$, $v_0 = 0.2$ and: (a) case A : $\gamma = 0.0$, (c) H : $\gamma = 0.01$ and (e) D : $\gamma = 0.01$. Mean values of the velocity (b), (d) and (f) calculated over 3000 trajectories related with the three case (a), (c) and (e), respectively. We call to attention that the order of magnitude from $\langle V \rangle$ changes drastically between cases A ; H ; D .

and Lieberman [3, 4], where the harmonic force was considered. An interesting behavior appears when the deformed sawtooth is introduced. For a very small asymmetry $\epsilon = 0.01$ (case H), the phase space is totally filled and no regular islands are observed [Fig. 2 (c)]. The corresponding $\langle \dot{v} \rangle$ increases very fast until $\langle \dot{v} \rangle \approx 10^1$ [see Fig. 2 (d)], showing that the accelerated mode is enhanced (hyperaccelerated) when compared to the case A. Another kind of motion occurs when $\epsilon = -0.01$ (case D) where many regular islands appear in phase space [see Fig. 2 (e)] which again prevent the acceleration to increase without bounds, as in case A. The corresponding $\langle \dot{v} \rangle$ remains almost constant for this example [Fig. 2 (f)]. A relevant property of case D is that: if the initial condition for the velocity is very high, the particle is decelerated. In other words, the hyperaccelerated particles from case D start to decelerate up to the time they reach the regular islands from Fig. 2 (e), but now from above. Therefore, there is a regular island barrier which prevents particles to decelerate until zero for short times. For very long times, however, particles may pass between the regular islands and decelerate to zero velocities. Such motion close to regular islands may lead to "sticky" or trapped [22] trajectories which affect the velocity and the convergency of the finite time Lyapunov exponents [23, 24, 25, 26].

In order to explain the effect of the deformed sawtooth pulse, we rewrite maps (1) and (2) in the very high velocity regime ($V_0 \gg 1$). In this case the time evolution for the phase can be neglected and we have

$$V_{n+1} = nV_0 \left(1 + \frac{j_0 - 1}{2} \right) : \quad (4)$$

From this expression for the velocity, we clearly see that when $\epsilon < 0$ the velocity is reduced by each iteration and the decelerated mode is obtained. When $\epsilon = 0$ the velocity is constant and when $\epsilon > 0$ the velocity increases without bounds and we get the hyperaccelerated case.

The above illustration shows the importance of a small deformation in the sawtooth wall motion on the dynamics in phase space and on the corresponding acceleration. Now we look at the stability of the trajectories for each situation A ; H ; D . Figure 3 shows the time evolution of the mean finite time Lyapunov exponent (LE), λ , calculated over 1000 trajectories for the three distinct cases A ; H ; D . The LEs are determined using the Benettin's method [27]. The full line shows λ for the case A , the long-dashed line for the case H and the dashed line for D . In the accelerate case A , λ is constant since every initial condition (with low velocity) is trapped inside the chaotic region of phase space. For the case D , the λ is almost constant, increasing very slowly. The time behavior of the mean LE in case D is similar to the mean LE from the A case in the following sense: the trajectory is trapped in the specific chaotic region in the phase space, below the islands of regularity [please compare Figs. 2 (a) and (e)]. For the hyperaccelerated case H (long-dashed line) the mean LE decreases almost to zero, showing that the filled space phase observed in Fig. 2 (c) is not chaotic. Albeit being not chaotic, no regular islands are observed, as in the other cases. This is apparently a typical behavior of linear unstable but ergodic systems [28], where besides having zero LEs the velocity space is totally filled.

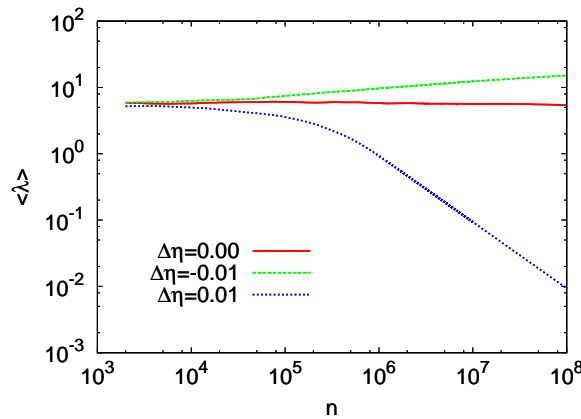


FIG. 3: Mean value of the Lyapunov exponent calculated over 1000 trajectories for the three situations: A : $\epsilon = 0.0$ (full line), D : $\epsilon < 0.0$ (dashed line) and H : $\epsilon > 0.0$ (long-dashed line).

At next we show how the Ratchetlike time asymmetry can be used to control the Fermi acceleration in order to get a desirable velocity. Figure 4 shows the time evolution of the particle velocity using a combination of cases H ; D

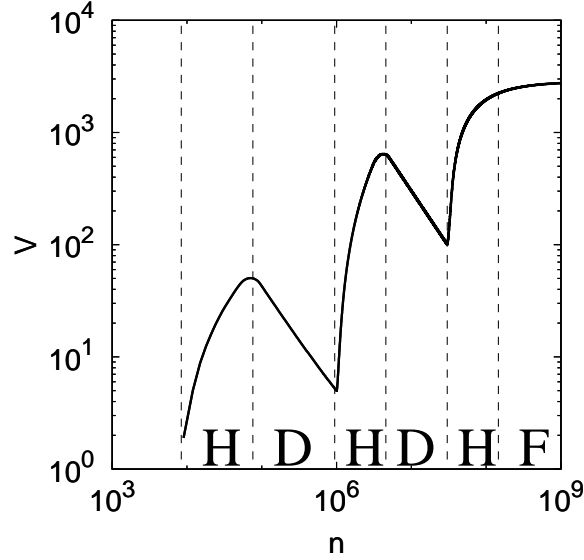


FIG. 4: Velocity as a function of the iteration n . It shows how the particles velocity can be controlled by switching the saw tooth pulse appropriately between cases H (hyperaccelerated) and D (decelerated), and finally F (fixed wall).

discussed above. While for the case H the hyperaccelerated mode is obtained, the case D is able to decelerate the particle velocity. When the desirable velocity is reached, the wall oscillation can be turned off (case F). By appropriately switching the Ratchetlike pulse between H/D modes, the velocity can be controlled. It is important to mention that the control is only possible due to the following particular property of the decelerated mode: the deceleration only occurs after the particle is hyperaccelerated, it does not occur for small velocities [see Fig. 2 (e)].

To conclude, for a long time the Fermi acceleration has been studied in different models and applications [1, 2, 3, 4, 5, 6, 7, 8, 9, 10, 11, 12, 13, 14, 15, 16, 17, 18, 19, 20]. However, none of these works (but one [10]) considered the possibility to control the particles in order to achieve a desirable velocity. Here we show the effect of a deformed sawtooth (Ratchetlike) pulse to control the particle velocity in the Fermi-Ulam model. Changing the asymmetry parameter from the Ratchetlike pulse we are able to get Fermi hyperacceleration and deceleration. In fact, the time integral of the pulse (the wall position) over one period of oscillation must be different from zero in order to get the control. When the mentioned integral is positive (negative), the Fermi hyperacceleration (deceleration) occurs. This allows us to, by switching the pulse between hyperacceleration and deceleration modes, to control the particles velocity. We also show that the decelerated and normal accelerated cases are chaotic, while for the hyperaccelerated case the LEs converge to zero. Additionally we give numerical evidences which indicate that the hyperaccelerated case is ergodic in velocity space. It would be interesting to observe the deformed sawtooth pulse to control the particle velocity in the presence of dissipation [29].

ACKNOWLEDGMENTS

The authors thank CNPq and FINEP (under project CTINFRA-1) for financial support.

E-mail address: cm.anchein@gmail.com

^y E-mail address: mbeim@fisica.ufpr.br

[1] E. Fermi, Phys. Rev. 75, 1169 (1949).

[2] S.M. Ulam (University of California Press, Berkely, 1961), vol. 3.

[3] M.A. Lieberman and A.J. Lichtenberg, Phys. Rev. A 5, 1852 (1972).

[4] A.J. Lichtenberg and M.A. Lieberman, Regular and Chaotic Dynamics (Springer-Verlag, 1992).

[5] E.D. Leonel, J.K.L. da Silva, and S.O. Kamphorst, Physica A 331, 435 (2004).

[6] E.D. Leonel, P.V.E.M. McClintock, and J.K.L. da Silva, Phys. Rev. Lett. 93, 014101 (2004).

- [7] E.D. Leonel and P.V.E.M. McClintock, *J. Phys. A* **38**, 823 (2005).
- [8] R.E. de Carvalho, F.C. Souza, and E.D. Leonel, *Phys. Rev. E* **73**, 066229 (2006).
- [9] A.K. Karlis, P.K. Papachristou, F.K. Diakonos, V. Constantoudis, and Schmelter, *Phys. Rev. Lett.* **97**, 194102 (2006).
- [10] A.K. Karlis, P.K. Papachristou, F.K. Diakonos, V. Constantoudis, and Schmelter, *Phys. Rev. E* **76**, 016214 (2007).
- [11] L.D. Pustyl'nikov, *Trudy Moskov. Mat. Obsc. Tom* **34**, 1 (1977) (*Trans. Moscow Math. Soc.* **2**, 1 (1978)).
- [12] A. Steane, P. Szriftgiser, P. Desbieres, and J. Dalibard, *Phys. Rev. Lett.* **74**, 4972 (1995).
- [13] F. Saif, I. Bialynicki-Birula, M. Fortunato, and W. P. Schleich, *Phys. Rev. A* **58**, 4779 (1998).
- [14] F. Saif, *Phys. Rep.* **419**, 207 (2005).
- [15] A.V. Mikhov and L.M. Zeleny, *Phys. Rev. E* **64**, 052101 (2001).
- [16] G. Michalek, M. Ostrowski, and R. Schickeiser, *Sol. Phys.* **184**, 339 (2001).
- [17] A. Veltri and V. Carbone, *Phys. Rev. Lett.* **92**, 143901 (2004).
- [18] K. Kobayakawa, Y. S. Honda, and T. Tamura, *Phys. Rev. D* **66**, 083004 (2002).
- [19] M. A. Malkov, *Phys. Rev. E* **58**, 4911 (1998).
- [20] D. Cole, S. Bending, S. Savelliev, A. Grigorenko, T. Tamegai, and F. Nori, *Nature Materials* **5**, 305 (2006).
- [21] L. Angelani, R.D. Leonardo, and G. Ruocco, *Phys. Rev. Lett.* **102**, 048104 (2009).
- [22] G.M. Zaslavski, *Phys. Rep.* **371**, 461 (2002).
- [23] M.W. Beims, C. Mainlein, and J.M. Rost, *Phys. Rev. E* **76**, 056203 (2007).
- [24] C. Mainlein and M.W. Beims, *Chaos, Solitons & Fractals* (2007), doi:10.1016/j.chaos.2007.06.112.
- [25] C. Mainlein, M.W. Beims, and J.M. Rost, submitted (2009).
- [26] J.D. Szezech, S.R. Lopes, and R.L. Viana, *Phys. Lett. A* **335**, 394 (2005).
- [27] G. Benettin, L. Galgani, A. Giorgilli, and J.-M. Strelcyn, *Meccanica* **15**, 09 (1980).
- [28] G. Casati and J. Ford, *J. Comp. Phys.* **20**, 97 (1976).
- [29] C. Mainlein and M.W. Beims, in preparation (2009).